

Multiple Large Inputs to Principal Cells in the Mouse Medial Nucleus of the Trapezoid Body

Jeremy B. Bergsman,^{1,2} Pietro De Camilli,² and David A. McCormick¹

¹Department of Neurobiology and ²Howard Hughes Medical Institute and Department of Cell Biology, Yale University School of Medicine, New Haven, Connecticut 06520-8001

Submitted 24 September 2003; accepted in final form 12 February 2004

Bergsman, Jeremy B., Pietro De Camilli, and David A. McCormick. Multiple large inputs to principal cells in the mouse medial nucleus of the trapezoid body. *J Neurophysiol* 92: 545–552, 2004; 10.1152/jn.00927.2003. The calyx of Held is a giant nerve terminal that forms a synapse directly onto the principal cells of the medial nucleus of the trapezoid body (MNTB) in the mammalian auditory brain stem. This central synapse, which is involved in sound localization, has become widely used for studying synaptic transmission. Anatomical studies of this nucleus have indicated that each principal cell is innervated by only one calyx. Here we use previously established electrophysiological criteria of excitatory postsynaptic current amplitude, kinetics, and transmitter type, as well as other characteristics commonly reported for this synapse, to examine the input properties of principal neurons. Our findings indicate that some principal cells receive more than one strong excitatory input. These inputs meet previously established electrophysiological criteria for identification as calyceal nerve terminals. Implications for the execution and analysis of experiments to avoid errors due to such multiple inputs are discussed.

INTRODUCTION

The largest presynaptic terminal in the mammalian CNS is the calyx of Held (Morest et al. 1973), which forms an excitatory axosomatic synapse on the principal cells of the medial nucleus of the trapezoid body (MNTB). Because both the presynaptic terminal and postsynaptic cell are amenable to patch-clamp recording (Forsythe 1994; Forsythe and Barnes-Davies 1993b), this synapse has rapidly become a widely used model system for studying many aspects of synaptic transmission.

The architecture of the MNTB has been characterized anatomically at light and electron microscope levels. Axons from the globular bushy cells in the ventral cochlear nucleus (VCN) cross the midline in the trapezoid body and give rise to one or two calyces (Smith et al. 1991). Anatomical studies in the young and mature rat (Casey and Feldman 1985; Kandler and Friauf 1993; Sätzler et al. 2002; Taschenberger et al. 2002), cat (Morest 1968a; Smith et al. 1991), and other animals (e.g., Lenn and Reese 1966) have reported that each postsynaptic principal cell receives input from only one calyx. In addition to the calyceal synapse, other, smaller, bouton contacts onto the principal cell and its dendrites have been observed (e.g., Lenn and Reese 1966). One study in the cat indicated that the small contacts may cover as much of the principal cell as the calyx (Smith et al. 1991) although most studies have reported a lower fraction. These contacts have been distinguished from calyceal

contacts by the size and type of vesicles they contain and the curvature and symmetry (or lack thereof) of the active zones. Most of these small contacts are thought to be GABAergic or glycinergic (Smith et al. 1998) and did not appear to arise from the axons giving rise to calyces, with only $\leq 5\%$ attributable to so-called “calycine collaterals”—boutons extending from calyces on neighboring principal cells (Jean-Baptiste and Morest 1975; Morest 1968a,b, 1973; Morest et al. 1973; Smith et al. 1991). Without serial sectioning and extensive reconstruction, it is difficult to determine whether such contacts might originate from a calyceal process and whether all calyceal contacts truly arise from a single structure. Accordingly, it has been hypothesized that occasional instances of high calyceal-type coverage of MNTB principal cells may result from innervation by two calyces (Smith et al. 1998).

Electrophysiological recordings have reinforced the anatomical findings, showing that in addition to the large excitatory input ascribed to the calyx of Held, there are other, smaller excitatory and inhibitory inputs to the principal cells in the MNTB (Banks and Smith 1992; Forsythe and Barnes-Davies 1993a; Hamann et al. 2003). Criteria have been published for distinguishing calyceal from noncalyceal inputs in electrophysiological experiments. Inhibitory inputs are easily separated by the use of specific blockers of neurotransmitter receptors. For the excitatory inputs, Banks and Smith distinguished noncalyceal inputs by their greatly increased latency and their graded responses to stimulation strength. Similar properties of the small excitatory inputs were noted by Hamann et al. Another criterion used to distinguish likely calyceal from noncalyceal inputs was those excitatory postsynaptic currents (EPSCs) >391 pA versus those <196 pA (after correcting for the difference in holding potential to -80 mV) (Barnes-Davies and Forsythe 1995; Forsythe and Barnes-Davies 1993a). Another group has used a higher cutoff value (>1 nA) (Futai et al. 2001; Ishikawa et al. 2003). However, when the excitatory inputs are stimulated by afferent fiber stimulation, the experimenter has no information about the morphology of the large input. Because differences between the evoked responses in such experiments and those in paired pre- and postsynaptic recordings have not been reported, the most parsimonious explanation is that these large responses are due to the calyx input.

Here we report whole cell patch-clamp recordings from principal cells in the mouse MNTB that received more than one large, all-or-none, excitatory input. Each input had all the

Address for reprint requests and other correspondence: J. Bergsman, Department of Neurobiology, P.O. Box 208001, New Haven, CT 06520-8001 (E-mail: jeremy@bergsman.org.)

The costs of publication of this article were defrayed in part by the payment of page charges. The article must therefore be hereby marked “advertisement” in accordance with 18 U.S.C. Section 1734 solely to indicate this fact.

electrophysiological characteristics ascribed to the calyceal inputs to these cells, suggesting that some cells may receive multiple calyces as described anatomically in the ventral cochlear nucleus (Lenn and Reese 1966). In the 101 cells we examined for the occurrence of this phenomenon (after the cell in which we first noticed it serendipitously), we identified it in six more cells; as discussed in the following text, this may represent an underestimate of the true frequency. Therefore multiple inputs are present in young mice and are an important factor in the execution and interpretation of experiments at this synapse.

METHODS

Slice preparation

P7 to P12 C57BL/6, C57BL/6X129SV, or BALB/c/Weeble (Nystuen et al. 2001) mice were decapitated in accord with Yale's IACUC policies, and the brain stems were rapidly transferred to ice-cold low-Ca²⁺ artificial cerebrospinal fluid (ACSF) containing (in mM) 125 NaCl, 2.5 KCl, 25 NaHCO₃, 1.25 NaH₂PO₄, 25 dextrose, 0.1 CaCl₂, 3 MgCl₂, 3 myo-inositol, 2 sodium pyruvate, and 0.4 ascorbic acid bubbled with 95% O₂-5% CO₂. Transverse brain stem slices (200–210 μm) were cut rostral to the seventh nerve. Careful orientation of the plane of sectioning was important to maximize the number of connected cells. Slices were cut at a slight (~5°) angle relative to the medial-lateral axis such that the axons giving rise to the calyces of Held ran up through the slice to the MNTB on one side, and recordings were only made from this side (see supplemental Fig. 1¹). The dorsal-ventral axis was also controlled such that the rostral extent of the fourth ventricle was sliced with the ventro-rostral extent of the seventh nerve in the brain stem. Slices were immediately transferred to normal Ca²⁺ ACSF (as in the preceding text with 2 mM CaCl₂ and 1 mM MgCl₂) and held at 35°C for 40–50 min and at room temperature thereafter until they were used.

Electrophysiology

Slices were placed in a perfusion chamber (RC-26G Warner Instruments, Hamden, CT) on a Zeiss (Germany) Axioskop 2 microscope and visualized with a ×40 water-immersion lens and video (Hamamatsu C400-79H camera and C2400 controller) infrared differential interference microscopy. Slices were continuously perfused with ACSF warmed to 26°C (Warner SH-27A) at ~1 ml/min. ACSF contained 25 μM D-2-amino-5-phosphonovaleric acid, 10 μM (-)-bicuculline methiodide 1S9R, and 500 nM strychnine HCl to block N-methyl-D-aspartate (NMDA), GABA, and glycine receptors respectively.

Patch pipettes were pulled (P97, Sutter Instruments, Novato, CA) from leaded glass capillaries [PG10165 World Precision Instruments (WPI), Sarasota, FL] and had a tip resistance of 1.5–2.5 MΩ when filled with an internal solution containing (in mM) 110 CsF, 30 CsCl, 5 EGTA, 10 HEPES, and 2 QX-314, adjusted to pH 7.3 with CsOH and to 295 mosM with H₂O. After obtaining the whole cell configuration, the series resistance was usually <7 MΩ, and experiments were discarded if the series resistance was >10 MΩ or changed significantly during the experiment. Experiments were also discarded if the leak conductance was >5 nS. Series resistance was compensated by 80% with a lag of 10 μs using the built-in functions of the Axopatch 200B amplifier (Axon Instruments, Foster City, CA). The holding potential was -80 mV except for reversal potential experiments. No correction was made for the liquid junction potential, which was estimated to be ~7 mV. Axons giving rise to the calyces

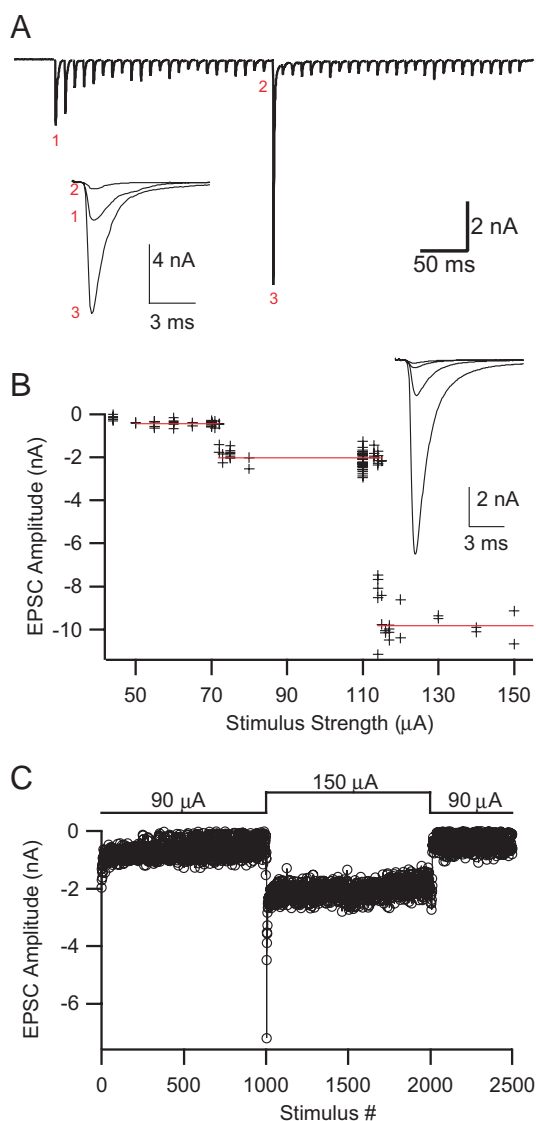


FIG. 1. Multiple inputs to medial nucleus of the trapezoid body (MNTB) principal cell. *A*: postsynaptic current recorded during a 100-Hz, 50-stimulus train elicited by 110-μA pulses. Responses marked 1–3 are expanded in *inset* where they are time aligned to the stimulation. Stimulus artifacts were blanked for clarity. *B*: excitatory postsynaptic current (EPSC) amplitude as a function of the strength of single stimuli. Red lines indicate average response levels for the stimulus ranges described in the results. *Inset*: averages of 4–6 EPSCs at 44, 60, 75, and 117 μA time aligned to the stimulation. *C*, *bottom*: EPSC amplitudes in response to a 30-Hz train. *Top*: stimulation strength. Many failures occurred at 90 μA—this is common with extended high-frequency stimulation near the threshold (data not shown).

of Held were stimulated via a bipolar electrode (15–30 kΩ typical impedance, FHC, Bowdoinham ME) positioned just ipsilateral to the midline of the trapezoid body by delivering brief (0.15 ms) constant current pulses. Stimulation was triggered by Clampex 8.2 (Axon Instruments) protocols through a Master 8 timer (AMPI, Israel) connected to a stimulus isolator (A360, WPI).

Cell selection

A glass micropipette was used as an extracellular electrode to search for cells on or near the surface of the slice that received input evoked by stimulation (Borst et al. 1995). We began our search for cells on the lateral side of the MNTB, which might have biased our

¹ The Supplementary Material for this article (a figure) is available online at <http://jn.physiology.org/cgi/content/full/000927.2003/DC1>.

recordings for cells on this side, which receive input from globular bushy cells with a lower characteristic frequency due to the tonotopic organization of this nucleus (Guinan et al. 1972; Smith et al. 1998). Slices varied in their fraction of connected cells, from ~1 in 2 to ~1 in 30.

Data analysis

Currents were filtered at 2–5 kHz and digitally sampled (Digidata 1322A Axon Instruments) at 10–25 kHz and recorded on a PC running Clampex. Data were analyzed off-line in Igor Pro 4 (Wave-metrics, Lake Oswego, OR) and Microsoft Excel 2000 (Microsoft, Redman, WA) and expressed as means \pm SD. EPSC amplitudes were computed as the peak current during the EPSC after subtraction of the baseline current immediately preceding the stimulation.

Chemicals

QX-314 was from Alomone Labs (Israel), bicuculline was from RBI (Natick, MA) major bath constituents were from JT Baker (Phillipsburg, NJ), and other chemicals were from Sigma (St. Louis, MO).

RESULTS

MNTB principal cell with three large inputs

We first noticed an instance of multiple large inputs during a voltage-clamp recording of an MNTB principal cell. First we present the properties of this exemplary cell in detail and then compare it to the recordings of other cells with multiple inputs, which were mostly similar. A bipolar electrode was used to apply 110- μ A pulses to stimulate the axons leading to the MNTB as they crossed the midline of the brain stem in the trapezoid body (Forsythe and Barnes-Davies 1993a) while we measured EPSCs in this cell. A train of 50 stimuli at 100 Hz produced the well-described presynaptic depression of the EPSC amplitude (Fig. 1A) (e.g., Borst et al. 1995). However, after the depression reached a steady state, one EPSC was much larger than the steady-state amplitude (response marked 3 in Fig. 1A). In fact, it was much larger than even the initial nondepressed EPSC.

Systematic variation of the stimulus strength applied to the bipolar electrode revealed three different EPSC size ranges in this cell (Fig. 1B). Below 50 μ A little response was seen. Between 50 and 70 μ A, the response averaged 0.44 nA. Stimulation between 72 and 113 μ A elicited EPSCs with amplitudes of ~2 nA. Any stimulation >115 μ A elicited EPSCs with an average amplitude of 9.8 nA. Thus this cell appeared to have at least three inputs. Presumably the larger EPSC amplitudes included the EPSCs elicited with lower stimulation strengths, so by subtraction, the three amplitudes were ~0.44, 1.6, and 7.8 nA (*cell A* in Table 1).

To confirm that the response to the higher stimulation strength was the sum of the lower- and higher-threshold inputs, we utilized a protocol that allowed us to measure the response to the high-threshold input in relative isolation (Fig. 1C). We first stimulated at 30 Hz at 90 μ A—the middle of the medium-threshold range. After ~1,000 stimuli, the EPSCs elicited by the medium- and low-threshold inputs were depressed to a low level (0.56 nA, 28% of their initial value). During continued 30-Hz stimulation, the stimulus strength was increased to 150 μ A, significantly above the high-threshold level. The first EPSC after the increase in stimulus strength was 7.2 nA and presumably represented an undepressed high-threshold input in addition to the 0.56-nA depressed response of the low and middle inputs. The EPSCs containing the high-threshold input also quickly depressed to a steady state, which was maintained for another 1,000 stimuli. Returning the stimulus strength to 90 μ A reduced the response to slightly less than the steady state that had previously been reached at this stimulus level (0.36 nA). In three such trials (1 at 100 Hz) in this cell, the first large EPSC averaged 7.5 ± 1.0 nA larger than the depressed responses preceding it, in accord with the previous estimate for the size of the high-threshold input.

All inputs mediated by AMPA receptors

The neurotransmitter released by the calyx of Held onto the principal neuron is glutamate (Banks and Smith 1992; Wu and Kelly 1992). Released glutamate activates AMPA and, depending on the age of the animal (Futai et al. 2001; Taschenberger

TABLE 1. Characteristics of cells with multiple large inputs

| Cell | Age, d | Strain | Stimulation Threshold, μ A | EPSC Amplitude ^a nA | Maximum Frequency ^b (Hz) | Latency ^c (ms) |
|------|--------|----------------------------|--------------------------------|--------------------------------|-------------------------------------|---------------------------|
| A | 10 | C57BL/6 | 50 | -0.44 ± 0.12 | Not tested | 2.1 ± 0.1 |
| | | | 72 | -1.6 ± 0.4 | 300 ^d | 2.2 ± 0.1^d |
| | | | 115 | -7.8 ± 0.6 | 300 | 2.2 ± 0.05 |
| B | 7 | C57BL/6 \times 129SV | 365 | -5.1 ± 0.5 | ≥ 100 | 2.6 ± 0.08 |
| | | | 500 | $-3.5 \pm 0.6^*$ | Unreliable | 3.0 ± 0.2 |
| C | 10 | C57BL/6 \times 129SV | 240 | -2.3 ± 0.4 | ≥ 200 | 2.0 ± 0.07 |
| | | | 410 | -3.7 ± 0.5 | ≥ 100 | 2.5 ± 0.08 |
| D | 11 | C57BL/6 \times 129SV | 105 | -0.73 ± 0.23 | Not tested | 1.9 ± 0.07 |
| | | | 130 | -4.3 ± 2.2 | Not tested | 2.2 ± 0.05 |
| E | 12 | C57BL/6 | 215 | -1.1 ± 0.2 | Not tested | 2.2 ± 0.09 |
| | | | 225 | -3.7 ± 0.4 | ≥ 100 | 1.7 ± 0.04 |
| F | 9 | C57BL/6 \times 129SV | 365 | -2.5 ± 0.5 | Not tested | 2.2 ± 0.1 |
| | | | 565 | -3.9 ± 0.4 | Not tested | 2.1 ± 0.05 |
| G | 13 | BALB/c/Weeble ^e | 300 | -0.80 ± 0.02 | 200 | 2.0 ± 0.06 |
| | | | 450 | -5.9 ± 1.1 | 200 | 1.6 ± 0.1 |

Values are means \pm SD. ^aValue for high threshold inputs determined by subtracting the value of lower-threshold inputs except as indicated (*, see RESULTS). ^bHighest stimulation frequency at which no or very few failures were seen in 50 stimuli. Some cells were not tested to their limit. ^cTime from onset of the stimulus artifact to the peak of the excitatory postsynaptic current (EPSC); higher-threshold response latencies were measured after depression of the lower-threshold response(s). ^dIncludes lower-threshold response. ^eA null mutant in the gene for inositol polyphosphate 4-phosphatase type I (Nystuen et al. 2001)

and von Gersdorff 2000), NMDA receptors. In addition there are inhibitory inputs, presumably mediated by GABA and glycine (Banks and Smith 1992; Forsythe and Barnes-Davies 1993a). Because all our experiments were performed in the presence of GABA, NMDA, and glycine receptor blockers in the bath and fluoride in the pipette (see METHODS), the EPSCs described in the preceding text presumably were mediated by glutamate acting at AMPA receptors. To confirm this, we measured the reversal potentials of the low/middle- and high-threshold EPSCs (Fig. 2A). EPSCs were elicited during sustained depolarizations to a range of potentials from -60 to $+50$ mV. The AMPA receptor-mediated EPSCs at this synapse reverse at a holding potential of approximately $+9$ mV (less a 7-mV junction potential) (Forsythe and Barnes-Davies 1993a). We subtracted the currents evoked at the middle stimulus strength ($90 \mu\text{A}$; red circles) from those evoked at the same potential by the stronger stimuli ($150 \mu\text{A}$; open black circles)

to estimate the currents due to the higher threshold input alone (filled black circles). Linear fits to these data estimated reversal potentials of $+10$ mV for both inputs, supporting the idea that these currents were mediated by AMPA receptors. We also applied the AMPA receptor blocker CNQX ($10 \mu\text{M}$) during repeated, low-frequency (0.2 Hz) stimulation at $150 \mu\text{A}$, which blocked the EPSCs by 97% (Fig. 2B), indicating that all three responses were mediated by AMPA receptors. After removal of the CNQX, the EPSC amplitude gradually returned to 86% of the control level. Occasional reductions of the stimulation strength to $90 \mu\text{A}$ during the control, CNQX, and wash periods revealed that the larger two components were blocked similarly by the CNQX.

Classification of the inputs

The 0.44-nA, low-threshold response in *cell A* was smaller than the typical large EPSC seen in MNTB principal cells, which in our experiments typically ranged from 1 to 10 nA (mean = 3.9 ± 1.5 nA, $n = 23$). However, the presence of small inputs in addition to or instead of a large one is not uncommon in these recordings (Banks and Smith 1992; Forsythe and Barnes-Davies 1993a; Hamann et al. 2003) (see also following text). We considered whether this cell might somehow have an unusually large number of such small inputs with identical stimulation thresholds. To attempt to answer this question, we considered criteria that have been published for distinguishing calyceal from noncalyceal inputs (see INTRODUCTION). We measured the latency of the low-threshold input, the low- and middle-threshold inputs together, and the high-threshold input after depressing the lower-threshold inputs using the depression protocol depicted in Fig. 1C. The latencies in this cell differed by no more than 0.1 ms and by no more than 0.5 ms for any other example (Fig. 1B, inset, and Table 1), sharply distinguishing them from noncalyceal inputs according to the latency criterion described by Banks and Smith (an additional 2 ms at 33.5°C) (Banks and Smith 1992).

Some of our recordings, including some with multiple large inputs, did exhibit small inputs with longer, and typically more variable, latency. An example of this can be seen in Fig. 2C, which shows two responses of *cell G* to stimulation at each of two intensities. Stimulation at $350 \mu\text{A}$ produced a 0.8-nA EPSC. Stimulation at $525 \mu\text{A}$ recruited not only a 5.9-pA response with a similar latency to the response seen to $350\text{-}\mu\text{A}$ stimulation but also a small response with a latency >3 ms longer than the other two (Fig. 2C, arrow).

Another means to distinguish likely calyceal from noncalyceal inputs was a large EPSC amplitude. The criterion of the Forsythe group (391 pA) (Barnes-Davies and Forsythe 1995; Forsythe and Barnes-Davies 1993a), would again classify the 0.44 nA input in *cell A* as a calyx. However, we used lower-resistance electrodes and also low-pass filtered our data at a higher frequency before digitization, both of which would result in our recording larger responses. The criterion of the Takahashi group (>1 nA) (Futai et al. 2001; Ishikawa et al. 2003) would not classify this as a calyx input. We did not study further this small input, although it contributed to the currents elicited with higher-intensity stimulation.

Although the 1.6-nA, middle-threshold EPSC amplitude of *cell A* was on the low end of the range typical for these cells, it was still a substantial input, sufficient in principle to evoke

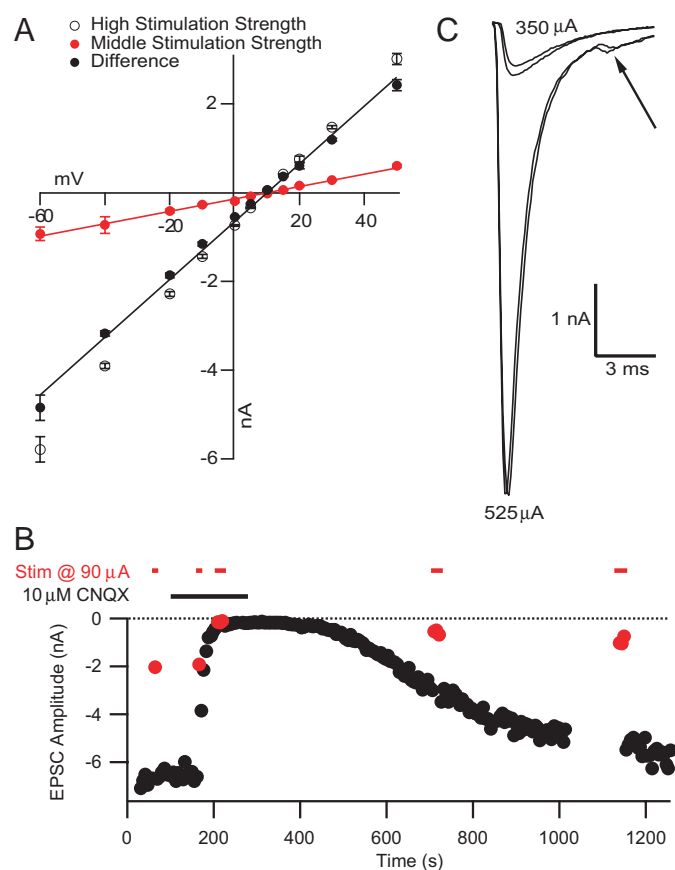


FIG. 2. Large inputs met criteria used to identify the calyx of Held. *A*: amplitudes of EPSCs (peak – baseline) elicited at various holding potentials (maintained for 15 ms before and 10 ms after stimulation) were used to estimate the reversal potential of the currents in *cell A*. Red symbols: EPSCs evoked at $90 \mu\text{A}$; open symbols, EPSCs evoked at $150 \mu\text{A}$; black symbols: the difference between the responses to high and middle strength stimulation. Each point is the average of 3 measurements and error bars represent the SDs. Black and red lines, linear regressions to the corresponding data. *B*: 6-cyano-7-nitroquinoxaline-2,3-dione (CNQX) blocked both larger- and smaller-amplitude EPSCs in *cell A*. Responses evoked by 0.2-Hz stimulation at $150 \mu\text{A}$ except for EPSCs elicited at $90 \mu\text{A}$, indicated by red symbols and bars at the top. CNQX application ($10 \mu\text{M}$) indicated by the black bar. *C*: 2 responses each to stimulation at 350 or $525 \mu\text{A}$ in *cell G*. Responses are time aligned to the stimulation. The latency of the large responses at each stimulation strength were similar, but a small, long-latency response was also present with stimulation at $525 \mu\text{A}$ (arrow).

an action potential in the principal cell (Brew and Forsythe 1995; Wang et al. 1998), although the presence of QX-314 in the recording pipette prevented testing this directly in this cell. This and the larger, highest-threshold input both met the published criteria of amplitude, latency, nongraded responses to stimulation strength, and transmitter type for identification as originating from a calyx. Other characteristics that supported this identification were their ability to follow very high-frequency stimulation (Table 1) and the nature of their short-term plasticity (see following text).

Comparison of the larger inputs' short-term plasticity

We next compared the short-term plasticity of the two larger synaptic inputs to *cell A*. Averaged responses to a middle stimulation strength were subtracted from the responses to a high stimulation strength to reveal the properties of the high-threshold input in isolation. Figure 3A shows the EPSC amplitudes in response to 100-Hz trains of 50 stimuli for the low/middle- and high-threshold inputs. Although the high-thresh-

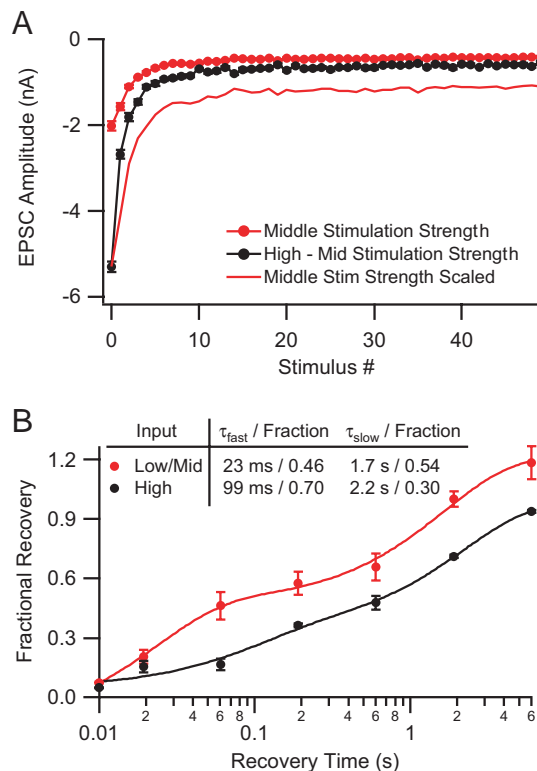


FIG. 3. Depression and recovery in MNTB principal *cell A*. *A*: EPSC amplitudes for a 100-Hz train of 50 stimuli. The average responses to the middle stimulus strength (78–110 μ A) are shown with red circles ($n = 31$). These values were subtracted from the average responses to high stimulation strength (150 μ A, $n = 18$), and the differences are shown with black circles. Some middle stimulation strength trials contained occasional large responses and were discarded. The red line without symbols depicts scaled middle stimulation strength responses. Error bars in both panels depict the SE of the averaged values. *B*: ratio of the EPSC amplitude after a period of recovery to the amplitude of the 1st EPSC in the train, plotted against the time of recovery. Symbols as in *A*; averages of 3–6 measurements. Lines are double exponential fits to the data. Time constants of the recovery and the corresponding fractional amplitudes are given in the figure. Trains were given every 40 s and only one recovery point was measured for each train. Most data were collected after wash off of CNQX (see Fig. 2*B*), and responses were smaller than responses before CNQX application.

old input started off almost three times as large as the low/middle-threshold inputs combined, it reached a similar steady-state response level after 8–10 stimuli. Scaling the responses to the middle stimulation strength to the high stimulation strength according to the size of the first response clearly revealed the difference in steady-state depression (Fig. 3*A*). This is a general property of this synapse (von Gersdorff et al. 1997).

We examined the recovery from this depression by giving a single stimulus at various times after completion of the 50 stimulus train. The response was normalized to the response to the first stimulus of the depressing train. This analysis revealed that the lower-threshold response recovered more quickly than the higher threshold response (Fig. 3*B*). The recovery rates were somewhat faster than those previously published for the mouse (Wang and Kaczmarek 1998), possibly due to the increased temperature and/or much longer depressing trains causing increased $[Ca^{2+}]_i$, which speeds recovery (Wang and Kaczmarek 1998). Analogous data were obtained with 50 stimulus trains at 50, 200, and 300 Hz (not shown). As previously shown, higher-frequency stimulation during depression resulted in more rapid recovery (Wang and Kaczmarek 1998). For each frequency of depressing train, the lower-threshold input recovered more rapidly than the higher-threshold one. Despite the substantial difference in the behavior of these inputs, results for both large inputs were within the normal range for cells with only one apparent input (data not shown).

Other examples of multiple inputs

After this recording, we systematically varied the stimulus strength in all of our subsequent recordings. All cells were tested with stimulation strengths ranging from threshold for eliciting a response over ~ 0.2 nA to approximately three times this threshold but always to ≥ 300 μ A. In the 101 recordings tested in this manner, six more gave evidence of more than one large input. The phenomenon was observed across the entire age range studied and in both an inbred and a hybrid strain. *Cells C–G* were much like *cell A* and will not be described further except for the details listed in Table 1. One recording (*B* in Table 1), however, gave larger responses to stronger stimulation only infrequently. A plot of the EPSC amplitude as a function of the strength of single stimuli is given in Fig. 4*A*. In this case, single stimuli did not clearly indicate the presence of multiple inputs, even when tested over a wide range of intensities. Only when the lower-threshold input was depressed from high-frequency stimulation was the presence of a second input clear. For example, a 100-Hz train at 450 μ A (Fig. 4*B*, *top*) resulted in typical depression, with two failures, to the second and fourth stimuli. An identical train with a stimulation strength of 550 μ A resulted in a similar depression, with no failures and occasional large undepressed EPSCs superimposed on the depressed lower threshold EPSCs (Fig. 4*B*, *bottom*). Because the higher-threshold input was weaker than the lower-threshold input (in contrast to *cell A*) and was so unreliable, we used the method depicted in Fig. 1*C* to depress the response to the lower-threshold input to estimate the size of the higher-threshold EPSC. The value obtained in this manner is reported in Table 1.

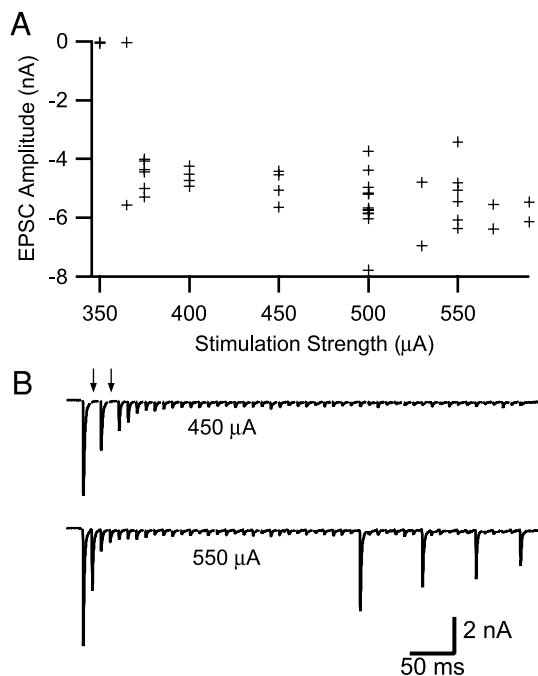


FIG. 4. Properties of MNTB principal cell *B*. *A*: EPSC amplitude vs. stimulus strength. *B*: postsynaptic currents during a 100-Hz, 50-stimulus train elicited by 450- μ A (*top*) or 550- μ A (*bottom*) stimulation. Stimulation artifacts were blanked for clarity. \downarrow , failures in response to the 2nd and 4th stimuli (*top*).

DISCUSSION

We have shown that a small fraction of principal cells in the mouse MNTB exhibit multiple discrete EPSC amplitudes in response to afferent fiber stimulation, consistent with innervation by multiple calyces of Held. We considered possible sources for variable response size other than multiple large inputs. EPSCs in these cells are large, and voltage clamping them can be difficult. If increasing the stimulus strength recruited a small input, this might have put the EPSC over the threshold for triggering a postsynaptic action potential. However, the inclusion of the voltage-gated sodium channel blocker QX-314 in the recording pipette prevented postsynaptic action potentials in all the recordings presented in this work. We could also be confident that escaping action potentials were not the cause of the larger responses because such unclamped currents would have been expected to surmount the strongest EPSCs, not the small, depressed responses (see Fig. 1, *A* and *C*). In any case, the linear current-voltage relationship of the responses (Fig. 2*A*) indicates that voltage-gated sodium channels were not activated. If sodium channels had contributed to the responses at -80 mV, the difference would have disappeared at depolarized potentials; this would have inactivated the sodium channels. For these reasons, we ruled out the involvement of sodium channels. We also considered whether greater stimulation strength might have recruited other fibers that worked through other neurons to somehow disinhibit or enhance transmission (pre- or postsynaptically) at the synapse under study. We rejected this hypothesis because it seemed unlikely that such an effect would have resulted in the same absolute amplitude increase to a depressed EPSC (Fig. 1*C*) as it did to an undepressed EPSC (Fig. 1*B*). Additionally there is no evidence for modulation through such a pathway. In fact,

the direct effect of small-amplitude, high-latency excitatory inputs onto principal cells has been suggested to inhibit postsynaptic responsiveness to the calyx input (Hamann et al. 2003). Thus the data presented here indicated that these cells received multiple large excitatory inputs. These inputs met commonly used electrophysiological criteria for classification as originating from the calyx of Held (Barnes-Davies and Forsythe 1995; Forsythe and Barnes-Davies 1993a; Futai et al. 2001).

Without retrospective anatomical studies we could not be sure that the inputs were calyces; however, their large amplitudes implied that whatever their form they must have covered a significant amount of the cell surface. Most MNTB principal cells have small dendritic arbors (Sommer et al. 1993), arguing against the possibility of a large collection of small dendritic contacts arising from a single axon or from a group of axons with extremely similar activation thresholds and other properties. We attempted to specifically load the terminals with the AM ester of a Ca^{2+} indicator by focally perfusing the axons as they crossed the midline (Regehr and Atluri 1995) to allow imaging of the structures excited by the afferent fiber stimulation. Unfortunately either the axons did not readily trap the dye, in agreement with previously published work (Billups et al. 2002), or the calyx volume was too large to load with this method. Definitive determination of the physical form of these inputs awaits anatomical experiments with the power to detect these uncommon occurrences with reasonable likelihood. Perhaps the most promising approach would be injection of a tracer and EM analysis of the calyces (Smith et al. 1991); this might reveal both labeled and unlabeled calyceal contacts on the same cell.

Other instances of cells that receive strong inputs from single neurons in mature animals, such as the neuromuscular junction onto skeletal muscle, the climbing fiber-Purkinje cell synapse in the cerebellum, and the neurons in the submandibular ganglion initially show innervation by multiple neurons before synapse elimination in the second and third postnatal week (in the rat) results in a single input (Brown et al. 1976; Crepel et al. 1976; Lichtman 1977). Afferent and efferent connections of the MNTB are also changing during this age (Kandler and Friauf 1993; Kim and Kandler 2003; Kuwabara et al. 1991), which is the age used for patch-clamp studies. If indeed some MNTB principal cells do receive multiple calyces, it will be important to determine whether this is a transitory phenomenon during development like that seen in the other instances of strong single inputs or whether it persists in adulthood. If this is a transitory phenomenon, it may prove to be a useful system for studying competition between inputs during development. Conversely if the existence of multiple large inputs is a persistent phenomenon, it will be important to determine whether it is sufficiently common to impact the processing of auditory information. Multiple inputs might increase the ability of the bushy cells in the VCN to synchronously drive the cells in the MNTB, as proposed for the endbulb of Held-bushy cell synapse (Joris et al. 1994). This is in line with the emerging idea that the MNTB principal cell is not simply a faithfully firing inverting relay but is subject to important noncalyceal inputs, which are integrated with the calyceal input to determine the postsynaptic firing pattern (Hamann et al. 2003; Kopp-Scheinplugg et al. 2003).

We found that careful orientation of the tissue during sectioning resulted in a relatively high fraction of MNTB cells on the surface of the slice retaining enough of their axons to be stimulated by the electrode placed at the midline of the slice (see METHODS). It was possible that this may have increased the number of cells in which we were able to stimulate more than one input compared with studies with a lower fraction of connected cells. Nevertheless, assuming all principal cells received calyceal input, we were rarely able to stimulate even half of the calyces near the surface of the slice. This implied that the fraction of cells that received multiple inputs may have been higher than our data indicated. If axons heading for the same cell ran together through the trapezoid body, they may have had similar outcomes from the cutting procedure and the underestimate may be small; but if there was variation in the axons' paths, the estimate could be low by a factor of two or more. Interestingly, such variation in axon course was cited as a biasing factor in the underestimate of the number of endbulbs of Held that converge on the bushy cells in the VCN (Ryugo and Sento 1991). It was also possible that instances of multiple inputs to MNTB cells with similar stimulation thresholds were not detected. If both inputs were reliable at the stimulation frequencies used, this situation would have been difficult to detect. In the other extreme, where one input is very unreliable, like that in Fig. 4, multiple inputs may be missed unless repeated stimulation is applied.

The potential presence of multiple large inputs should be taken into consideration when performing experiments at this synapse that utilize afferent fiber stimulation. Many parameters of synaptic transmission are quite variable from calyx to calyx at this developmental stage. Examples of such parameters include decay of residual Ca^{2+} and facilitation (Felmy et al. 2003), reliability in following high-frequency trains (Taschenberger et al. 2002), rate of depression following such trains (von Gersdorff et al. 1997), and recovery from this depression (unpublished results). If the combined influence of multiple inputs is measured, the results will be different from those expected for a single input as shown for depression and recovery from depression in Fig. 3. The results may be even more misleading if different combinations of the inputs are evoked with each stimulus due to unreliability or differences in ability of the inputs to follow high-frequency stimuli as in the example shown in Fig. 4.

Our findings suggest two procedural safeguards in experiments of this type. First, to avoid unknowingly recording from cells receiving multiple inputs, the experimenter must test that the response size is constant with changing stimulation strength over a fairly broad range covering the stimulation frequencies used in the experiments as stimulus threshold depends on the frequency of stimulation. As shown in Fig. 4, even this is not a perfect test. Choosing stimulation rates that produce a high fraction of failures, even if such frequencies will not subsequently be used in the experimental paradigm, may be more likely to reveal an instance of multiple inputs by revealing one input when the other fails. In addition to these strategies for avoiding instances of multiple inputs, a second safeguard may be to avoid recordings with smaller EPSC amplitudes. The combination of the fact that several of the inputs seen in the cases of multiple inputs were small and the lack of anatomical evidence for multiple calyces begs the question whether these small inputs are simply one end of a spectrum of calyx sizes or

whether they have a different underlying structure, which would likely imply other functional differences. Because limiting recordings to those with amplitudes greater than, for example, 2.5 nA, is not very restricting, such a criterion seems a reasonable precaution. On the other hand, the fact that most of the multiple input cells had one small input may be a special case of competition between the inputs and not apply to principal cells receiving only one strong input. Experiments using simultaneous pre- and postsynaptic recording avoid most of the problems of multiple inputs, although it must be considered when monitoring spontaneous miniature EPSCs that they may not arise from the input being studied.

ACKNOWLEDGMENTS

We thank Dr. Henrique von Gersdorff and members of his laboratory for assistance with the MNTB preparation.

GRANTS

This work was supported by grants from Howard Hughes Medical Institute and National Institutes of Health.

REFERENCES

- Banks MI and Smith PH.** Intracellular recordings from neurobiotin-labeled cells in brain slices of the rat medial nucleus of the trapezoid body. *J Neurosci* 12: 2819–2837, 1992.
- Barnes-Davies M and Forsythe ID.** Pre- and postsynaptic glutamate receptors at a giant excitatory synapse in rat auditory brainstem slices. *J Physiol* 488: 387–406, 1995.
- Billups B, Wong AY, and Forsythe ID.** Detecting synaptic connections in the medial nucleus of the trapezoid body using calcium imaging. *Pflügers Arch Eur J Physiol* 444: 663–669, 2002.
- Borst JG, Helmchen F, and Sakmann B.** Pre- and postsynaptic whole-cell recordings in the medial nucleus of the trapezoid body of the rat. *J Physiol* 489: 825–840, 1995.
- Brew HM and Forsythe ID.** Two voltage-dependent K^+ conductances with complementary functions in postsynaptic integration at a central auditory synapse. *J Neurosci* 15: 8011–8022, 1995.
- Brown MC, Jansen JK, and Van Essen D.** Polyneuronal innervation of skeletal muscle in new-born rats and its elimination during maturation. *J Physiol* 261: 387–422, 1976.
- Casey MA and Feldman ML.** Aging in the rat medial nucleus of the trapezoid body. II. Electron microscopy. *J Comp Neurol* 232: 401–413, 1985.
- Crepel F, Mariani J, and Delhaye-Bouchaud N.** Evidence for a multiple innervation of Purkinje cells by climbing fibers in the immature rat cerebellum. *J Neurobiol* 7: 567–578, 1976.
- Felmy F, Neher E, and Schneggenburger R.** Probing the intracellular calcium sensitivity of transmitter release during synaptic facilitation. *Neuron* 37: 801–811, 2003.
- Forsythe ID.** Direct patch recording from identified presynaptic terminals mediating glutamatergic EPSCs in the rat CNS in vitro. *J Physiol* 479: 381–387, 1994.
- Forsythe ID and Barnes-Davies M.** The binaural auditory pathway: excitatory amino acid receptors mediate dual timecourse excitatory postsynaptic currents in the rat medial nucleus of the trapezoid body. *Proc R Soc Lond B Biol Sci* 251: 151–157, 1993a.
- Forsythe ID and Barnes-Davies M.** The binaural auditory pathway: membrane currents limiting multiple action potential generation in the rat medial nucleus of the trapezoid body. *Proc R Soc Lond B Biol Sci* 251: 143–150, 1993b.
- Futai K, Okada M, Matsuyama K, and Takahashi T.** High-fidelity transmission acquired via a developmental decrease in NMDA receptor expression at an auditory synapse. *J Neurosci* 21: 3342–3349, 2001.
- Guinan J, Norris B, and Guinan S.** Single auditory units in the superior olivary complex. *Int J Neuroscience* 4: 147–166, 1972.
- Hamann M, Billups B, and Forsythe ID.** Non-calyceal excitatory inputs mediate low fidelity synaptic transmission in rat auditory brainstem slices. *Eur J Neurosci* 18: 2899–2902, 2003.
- Ishikawa T, Nakamura Y, Saitoh N, Li WB, Iwasaki S, and Takahashi T.** Distinct roles of Kv1 and Kv3 potassium channels at the calyx of Held presynaptic terminal. *J Neurosci* 23: 10445–10453, 2003.

- Jean-Baptiste M and Morest DK.** Transneuronal changes of synaptic endings and nuclear chromatin in the trapezoid body following cochlear ablations in cats. *J Comp Neurol* 162: 111–134, 1975.
- Joris PX, Carney LH, Smith PH, and Yin TC.** Enhancement of neural synchronization in the anteroventral cochlear nucleus. I. Responses to tones at the characteristic frequency. *J Neurophysiol* 71: 1022–1036, 1994.
- Kandler K and Friauf E.** Pre- and postnatal development of efferent connections of the cochlear nucleus in the rat. *J Comp Neurol* 328: 161–184, 1993.
- Kim G and Kandler K.** Elimination and strengthening of glycinergic/GABAergic connections during tonotopic map formation. *Nat Neurosci* 6: 282–290, 2003.
- Kopp-Scheinpflug C, Lippe WR, Dorrscheidt GJ, and Rubsamen R.** The medial nucleus of the trapezoid body in the gerbil is more than a relay: comparison of pre- and postsynaptic activity. *J Assoc Res Otolaryngol* 4: 1–23, 2003.
- Kuwabara N, DiCaprio RA, and Zook JM.** Afferents to the medial nucleus of the trapezoid body and their collateral projections. *J Comp Neurol* 314: 684–706, 1991.
- Lenn NJ and Reese TS.** The fine structure of nerve endings in the nucleus of the trapezoid body and the ventral cochlear nucleus. *Am J Anat* 118: 375–389, 1966.
- Lichtman JW.** The reorganization of synaptic connexions in the rat submandibular ganglion during post-natal development. *J Physiol* 273: 155–177, 1977.
- Morest DK.** Auditory neurons of the brain stem. *Adv Otorhinolaryngol* 20: 337–356, 1973.
- Morest DK.** The collateral system of the medial nucleus of the trapezoid body of the cat, its neuronal architecture and relation to the olivo-cochlear bundle. *Brain Res* 9: 288–311, 1968a.
- Morest DK.** The growth of synaptic endings in the mammalian brain: a study of the calyces of the trapezoid body. *Z Anat Entwicklungsgesch* 127: 201–220, 1968b.
- Morest DK, Kiang NYS, Kane EC, Guinan J, and Godfrey DA.** Stimulus coding at caudal levels of the cat's auditory nervous system. II. Patterns of synaptic organization. In: *Basic Mechanisms in Hearing*, edited by Moller AR. New York: Academic, 1973, p. 479–504.
- Nystuen A, Legare ME, Shultz LD, and Frankel WN.** A null mutation in inositol polyphosphate 4-phosphatase type I causes selective neuronal loss in weebie mutant mice. *Neuron* 32: 203–212, 2001.
- Regehr WG and Atluri PP.** Calcium transients in cerebellar granule cell presynaptic terminals. [erratum appears in *Biophys J* 69: 729, 1995]. *Biophys J* 68: 2156–2170, 1995.
- Ryugo DK and Sento S.** Synaptic connections of the auditory nerve in cats: relationship between endbulbs of Held and spherical bushy cells. *J Comp Neurol* 305: 35–48, 1991.
- Sätzler K, Söhl LF, Bollmann JH, Borst JG, Frotscher M, Sakmann B, and Lübke JH.** Three-dimensional reconstruction of a calyx of Held and its postsynaptic principal neuron in the medial nucleus of the trapezoid body. *J Neurosci* 22: 10567–10579, 2002.
- Smith PH, Joris PX, Carney LH, and Yin TC.** Projections of physiologically characterized globular bushy cell axons from the cochlear nucleus of the cat. *J Comp Neurol* 304: 387–407, 1991.
- Smith PH, Joris PX, and Yin TC.** Anatomy and physiology of principal cells of the medial nucleus of the trapezoid body (MNTB) of the cat. *J Neurophysiol* 79: 3127–3142, 1998.
- Sommer I, Lingenhohl K, and Friauf E.** Principal cells of the rat medial nucleus of the trapezoid body: an intracellular in vivo study of their physiology and morphology. *Exp Brain Res* 95: 223–239, 1993.
- Taschenberger H, Leao RM, Rowland KC, Spirou GA, and von Gersdorff H.** Optimizing synaptic architecture and efficiency for high-frequency transmission. *Neuron* 36: 1127–1143, 2002.
- Taschenberger H and von Gersdorff H.** Fine-tuning an auditory synapse for speed and fidelity: developmental changes in presynaptic waveform, EPSC kinetics, and synaptic plasticity. *J Neurosci* 20: 9162–9173, 2000.
- von Gersdorff H, Schneggenburger R, Weis S, and Neher E.** Presynaptic depression at a calyx synapse: the small contribution of metabotropic glutamate receptors. *J Neurosci* 17: 8137–8146, 1997.
- Wang LY, Gan L, Forsythe ID, and Kaczmarek LK.** Contribution of the Kv3.1 potassium channel to high-frequency firing in mouse auditory neurons. *J Physiol* 509: 183–194, 1998.
- Wang LY and Kaczmarek LK.** High-frequency firing helps replenish the readily releasable pool of synaptic vesicles. *Nature* 394: 384–388, 1998.
- Wu SH and Kelly JB.** Synaptic pharmacology of the superior olivary complex studied in mouse brain slice. *J Neurosci* 12: 3084–3097, 1992.